Radiofrequency and 2.45 GHz electron cyclotron resonance H^- volume production ion sources

2016 New J. Phys. 18 105008

(http://iopscience.iop.org/1367-2630/18/10/105008)

New Journal of Physics
The open access journal at the forefront of physics

Deutsche Physikalische Gesellschaft DPG
IOP Institute of Physics

Published in partnership with: Deutsche Physikalische Gesellschaft and the Institute of Physics

OPEN ACCESS

RECEIVED
22 July 2016

REVISED
22 September 2016

ACCEPTED FOR PUBLICATION
13 October 2016

PUBLISHED
26 October 2016

PAPER

Radiofrequency and 2.45 GHz electron cyclotron resonance H^- volume production ion sources

O Tarvainen[1,3] **and S X Peng**[2,4]

[1] University of Jyväskylä, Department of Physics, PO Box 35 (YFL), FI-40500 Jyväskylä, Finland
[2] State Key Laboratory of Nuclear Physics and Technology & Institute of Heavy Ion Physics, School of Physics, Peking University, Beijing 100871, People's Republic of China
[3] Corresponding author of sections 1–5 and 7.
[4] Corresponding author of section 6.

E-mail: olli.tarvainen@jyu.fi **and** sxpeng@pku.edu.cn

Keywords: negative ion source, dissociative electron attachment, radiofrequency plasma discharge, electron cyclotron resonance

Abstract

The volume production of negative hydrogen ions (H^-) in plasma ion sources is based on dissociative electron attachment (DEA) to rovibrationally excited hydrogen molecules (H_2), which is a two-step process requiring both, hot electrons for ionization, and vibrational excitation of the H_2 and cold electrons for the H^- formation through DEA. Traditionally H^- ion sources relying on the volume production have been tandem-type arc discharge sources equipped with biased filament cathodes sustaining the plasma by thermionic electron emission and with a magnetic filter separating the main discharge from the H^- formation volume. The main motivation to develop ion sources based on radiofrequency (RF) or electron cyclotron resonance (ECR) plasma discharges is to eliminate the apparent limitation of the cathode lifetime. In this paper we summarize the principles of H^- volume production dictating the ion source design and highlight the differences between the arc discharge and RF/ECR ion sources from both, physics and technology point-of-view. Furthermore, we introduce the state-of-the-art RF and ECR H^- volume production ion sources and review the challenges and future prospects of these yet developing technologies.

1. Introduction

Negative hydrogen ions (H^-/D^-) play an integral role in accelerator based research and applications (H^-) as well as fusion experiments utilizing neutral beam injection (D^-) [1, 2]. H^- ions are utilized for small-scale tandem accelerators and they enable charge exchange injection [3] into circular proton accelerators or storage rings. H^- ions are also used by high-current cyclotrons, which are becoming increasingly popular in radioisotope production. In that case the charge exchange process increases the extraction efficiency of the accelerator in comparison to proton beam and, therefore, reduces the radiological hazards and minimizes the maintenance effort. The diversity of applications drives the development of H^- ions sources towards various directions. Most often pulsed accelerators require high peak currents while machines operated in continuous mode benefit most from increased maintenance interval of the ion source and temporal stability of the ion beam. In the following sections we summarize the current understanding of H^- volume production mechanism, discuss the reasoning of the development of radiofrequency (RF) and electron cyclotron resonance (ECR) H^- ion sources and present a short review of the state-of-the-art ion sources utilizing the afore-mentioned plasma heating mechanisms.

2. Volume production of H^-

Modern H^- plasma ion sources rely on two ion formation processes, resonant-tunneling ionization on low work function surfaces [4] and volumetric ionization occurring in the plasma discharge [5]. Only the volume production will be discussed hereafter.

Mounting evidence (see e.g. [6] and references therein) indicates that the volume production of H^- is predominantly due to dissociative electron attachment (DEA) to rovibrationally excited ground state H_2 molecules. The reaction is believed to proceed through an intermediate H_2^- decaying to negative H^- ion and neutral H atom, i.e.

$$H_2(X^1\Sigma_g^+, \nu'') + e \rightarrow H_2^-(^2\Sigma_g^+) \rightarrow H^- + H. \quad (1)$$

The DEA cross section to vibrationally cold ground state $H_2(X^1\Sigma_g^+, \nu'' = 0)$ molecules is desperately small (on the order of 10^{-21} cm^2 [7]) to account for the negative ion densities observed in hydrogen discharges or to be of any practical use for ion source applications. Fortunately, the cross section of the DEA process depends strongly on the internal energy of the diatomic molecule [8]. This is due to the increased probability of the compound state dissociating without autoionization at large internuclear distance. The internuclear distance is affected by vibrational motion of the atoms and rotational (centrifugal) stretching of the molecule. The effect of the vibrational excitation on the DEA cross section is found to be more significant in comparison to the rotational excitation [9]. The DEA cross section increases by more than five orders of magnitudes if the H_2 are vibrationally excited to $\nu'' \geqslant 5$ [7]. Even more importantly, the cross section increases with decreasing electron energy and peaks at the threshold energy of the process, which in turn decreases with increasing vibrational level being 1.5 eV for $\nu'' = 5$, for example [7]. Thus, it is evident that achieving a sufficient volumetric production rate of H^- for an ion source application first requires vibrational excitation of molecular hydrogen to $H_2(X^1\Sigma_g^+, \nu'' \geqslant 5)$ states acting as a 'precursor' for the DEA reaction with cold electrons.

There are several pathways for the vibrational excitation of H_2. Vibrational excitation and de-excitation rate of H_2 in collisions with low energy electrons, referred as e–V excitation [10], is high in low temperature hydrogen discharges. However, the most probable outcome of the e–V excitation reaction is $\Delta\nu'' = \pm 1$ resulting to an equilibrium at low vibrational levels ($\nu'' \leqslant 4$) [10, 11]. The predominant channel for the excitations of high vibrational levels in the plasma volume is electronic excitation to $B^1\Sigma_u^+$ and $C^1\Pi_u$ singlet states, followed by VUV-emitting radiative decay to high vibrational levels ($\nu'' \geqslant 5$) of the $X^1\Sigma_g^+$ ground state [12]. The threshold energy for the H_2 electronic excitation is on the order of 10eV depending on the initial and final vibrational levels of the transition and the process becomes efficient at electron energies of approximately $\geqslant$20 eV. The (ground state) non-equilibrium vibrational distribution [10, 11] results from the Franck-Condon transition probabilities [13] defined by the overlap of the wave functions of the $B^1\Sigma_u^+$ or $C^1\Pi_u$ and $X^1\Sigma_g^+$ state vibrational levels.

Another channel for vibrational excitation of the H_2 molecules is the interaction between hydrogen atoms or molecular H_2^+ and H_3^+ ions and (transition) metal surfaces of the plasma chamber[6, 14]. Surface recombination of gas phase atoms may recycle hydrogen atoms into vibrationally excited molecules [15]. Different recombination mechanisms of hydrogen atoms have been summarized in [16]. In the case of H_2^+ the vibrational excitation proceeds predominantly through the repulsive $b^3\Sigma_u^+$ triplet state. The surface interaction quenches the triplet state by Auger relaxation populating high vibrational levels of the resulting $H_2(\nu'')$ molecules [14]. In the case of H_3^+ the first step of the process is electronic recombination and subsequent dissociation of the compound H_3 molecule to H and vibrationally excited $H_2(\nu'')$ [14]. The relative importance of the volumetric and surface-induced vibrational excitation channels depends on the ion source design, namely the discharge volume and surface area, choice of surface materials and electron kinetics. The contribution of the surfaces on vibrational kinetics of H_2 molecules in ion source plasmas is poorly understood due to the multitude of reaction channels and the effect of surface impurities.

Although being a prerequisite for volumetric as well as contributing to the surface-induced vibrational excitation of H_2, high energy electrons are destructive for the H^- ions through electron detachment [7]. Hence, optimizing the pure volume production of H^- requires a delicate balance between two worlds; maximizing the vibrational excitation rate of H_2 in collisions with hot electrons and, at the same time, maximizing the DEA rate of cold electrons together with preventing the destruction of the resulting H^- by hot electron impact. Such situation can be achieved only by spatial tailoring of the electron energy distribution (EED) through mechanical design of the ion source as discussed in the following sections.

3. Electron heating in RF and ECR discharges

The majority of the first generation H^- ion sources [17] based on the volume production mechanism are arc discharge sources employing a biased thermionic cathode, e.g. a filament, to produce free electrons which are then accelerated by the cathode potential across the plasma sheath to sustain the discharge. These energetic 'primary' electrons deposit their energy in multiple inelastic collisions, i.e. ionization and electronic excitation of the H_2 gas. Such discharges are typically confined by a permanent magnet multi-cusp field. The cusp-confinement improves their power efficiency as the trapped hot electrons eventually thermalize with the cold 'secondary' electrons produced through ionization. It is important to keep in mind that once the electrons are

accelerated across the cathode sheath they are not actively heated. The EED in arc discharge plasmas therefore spans from very low energies up to the energy corresponding to the cathode bias forming a rather uniform distribution (see e.g. [18]). This accounts for the major difference between arc discharges and RF/ECR discharges from the physics point-of-view of optimizing the H^- volume production and the discharge power efficiency.

The main motivation to develop ion sources based on RF or ECR plasma discharges is to eliminate the apparent limitation of the cathode lifetime. Such discharges also provide an elegant solution to avoid contamination of the plasma chamber surfaces by the cathode material and possible impurities, therefore enabling the optimization of the surface properties for the production of vibrationally excited $H_2(\nu'')$ molecules.

The basic principle of the electron heating by RF or microwave radiation is to expose the electrons to a time-varying electric field accelerating a sufficient number of them to energies exceeding the ionization potential of H_2, thereby sustaining the discharge. There are several methods to introduce the time-varying electric field. The simplest solution is to connect a planar electrode immersed in the plasma to a source of RF radiation through an impedance matching network and position another grounded electrode at a suitable distance from the (RF-) biased plate, thus creating an electric field between them. Such capacitive discharges in which the electrons are heated by the potential difference between the high-voltage electrode and the plasma are widely used in plasma processing but not in ion sources. This is because the achieved plasma density is rather low, on the order of 10^{10} cm^{-3} at pressures relevant for H^- production [19], which inherently limits the negative ion density.

So-called inductively coupled RF discharges utilize an antenna, which can be either immersed into the plasma or placed behind an RF-transparent window facing the plasma, and is connected to the RF power source (oscillating typically at 1–100 MHz) through a matching network. The electric field accelerating the electrons in the plasma volume is induced by the alternating current of the antenna as described by Faraday's law

$$\vec{\nabla} \times \vec{E} + \frac{\partial \vec{B}}{\partial t} = 0, \tag{2}$$

where the magnetic field is proportional to the antenna current. The most common types of antennas are flat spirals and solenoid loops wound either at the end or around the plasma chamber as explained e.g. in [20–23] discussing RF-driven H^- ion sources. The plasma densities achieved in high-power inductive discharges can reach 10^{12} cm^{-3} order of magnitude at relevant pressure regime.

ECR discharges are based on stochastic heating of electrons by microwave radiation launched directly into the plasma chamber, typically from a waveguide. The resonant interaction between the electrons and the microwave electric field requires the presence of an external magnetic field in which the electron gyrofrequency ω_{ce} matches the (angular) frequency of the microwaves ω i.e.

$$\omega = \omega_{ce} = \frac{eB}{m_e}. \tag{3}$$

If the resonance condition is fulfilled, the electrons passing through the resonance zone in correct phase with respect to the microwave electric field gain sufficient energy to ionize the H_2 gas and sustain the plasma. The vast majority of ECR discharges intended for the production of singly charged ions operate at 2.45 GHz, which is the industrial standard of commercial magnetron-type microwave amplifiers. The given frequency corresponds to resonance field strength B_{ECR} of 87.5 mT. Thus, the required external magnetic field can be easily generated by either electromagnets or permanent magnets. The field topology is typically a solenoid field aligned with the axis of the ion source plasma. 2.45 GHz ECR discharges have been reported to reach plasma densities up to 10^{12} cm^{-3} order of magnitude implying that they operate in so-called overdense mode in which the natural plasma oscillation frequency exceeds the electron gyrofrequency (see e.g. [24]). In such condition the electron motion is strongly perturbed by collisions and their gyroperiod becomes longer than in the collisionless case [25], which in turn implies that the magnetic field strength in collisional high-density plasmas should exceed the resonance field to recover the synchronization between the electron motion and microwave electric field. It has been experimentally demonstrated that highest plasma densities are obtained when $B_{ECR} < B < 1.3B_{ECR}$ [26].

From the fundamental point-of-view RF and ECR discharges are largely similar, i.e. free electrons produced through ionization are actively heated within the plasma volume. The resulting EED is often considered Maxwellian. Nevertheless, two electron populations with temperatures of 1–5 eV and $\geqslant$10 eV can often be identified (see e.g. [27]) especially in ECR discharges where the cold electrons are produced by ionization and the hot electron component of the distribution is heated locally by the resonant interaction. The electrons heated by the electromagnetic field dissipate their energy in inelastic collisions (predominantly) with neutral H_2 molecules. The EED has a profound effect on the volume production of H^- as the volumetric rates of both, the vibrational heating through electronic excitation to singlet states and DEA, depend strongly on the electron energy [7]. Moreover, the volumetric dissociation rate through electronic excitation to triplet states depends strongly on the EED. The dissociation rate itself affects the atomic to molecular hydrogen fraction in the discharge and,

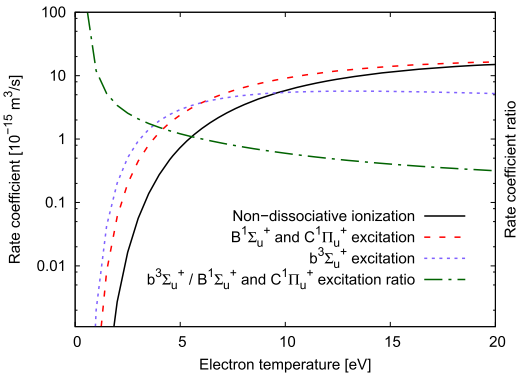

Figure 1. The rate coefficients as a function of (Maxwellian) electron temperature for (1) non-dissociative electron impact ionization from the ground state, (2) total electronic excitation to $B^1\Sigma_u^+$ and $C^1\Pi_u^+$ singlet states, which is proportional to the volumetric population rate of high vibrational levels of $H_2(\nu'' \geqslant 5)$, and (3) molecular dissociation via excitation to repulsive $b^3\Sigma_u^+$ triplet state together with (4) the ratio of the triplet and singlet state excitations.

therefore, plays a crucial role on plasma dynamics and surface processes. Figure 1 shows the rate coefficients $\langle \sigma v \rangle$ as a function of the electrons temperature for (1) non-dissociative ionization from the ground state, (2) total excitation to $B^1\Sigma_u^+$ and $C^1\Pi_u^+$ singlet states, directly populating high vibrational levels of $H_2(\nu'')$ through radiative decay back to the ground state, and (3) dissociation via excitation to repulsive $b^3\Sigma_u^+$ triplet state. The given electronic excitations contribute more than 80% to the total singlet and triplet excitation rates, respectively [7]. In the given example it is assumed that the H_2 molecules are vibrationally cold, i.e. their initial vibrational level is considered to be $\nu'' = 0$. The cross sections used for calculating the rate coefficients by numerical integration have been taken from [7]. Also the ratio of triplet to singlet excitation is plotted in the figure.

It can be deduced from the figure that electronic excitation to the repulsive $b^3\Sigma_u^+$ triplet state dominates over the other inelastic collisions (excluding the e–V vibrational excitation) if the electron temperature is < 6 eV, i.e. when the average electron energy $\langle E \rangle = 3/2kT_e$ is approximately 10 eV or less. This suggests that in RF and ECR discharges in which the majority of electrons have energies below 10 eV the efficiency of vibrational heating through singlet states is poor in comparison to arc discharges where the average hot electron energy is typically several tens of eV. In addition it can be expected that their hydrogen atom or proton fraction is more significant in comparison to arc discharge sources. The difference between the discharge types has been experimentally verified by comparing the volumetric rates of molecular ionization and excitation in an ECR discharge [28] and an arc discharge [29] indicating that the ionization and vibrational heating rates/kW of input power are higher in the arc discharge. Thus, from the H^- volume production point-of-view RF or ECR discharges cannot be expected to be as power efficient as arc discharge sources. However, since the contribution of surface processes to the volumetric rate of the DEA process is largely unknown, these ion source technologies could eventually be optimized in terms of power efficiency and atomic to molecular hydrogen fraction favoring H^- production through DEA. Altogether the obvious benefits of the cathode-less RF and ECR H^- ion sources warrant an extensive research effort summarized in the following sections.

4. Mechanical design of RF and ECR H^- volume production sources

The mechanical design of practically all volume production H^- ion sources, depicted schematically in figure 2, is based on division between (1) power delivery system (2) plasma heating volume, often referred as the driver-region or main discharge, (3) H^- production volume or filter region and (4) the extraction system.

The need for the division between the plasma heating and H^- production volumes arises from the conflicting nature of the two step volume production process, requiring both hot electrons for ionization and vibrational excitation of the H_2 molecules and cold electrons for the H^- formation through DEA. The main difference between the driver regions of RF and ECR ion sources is the necessity of a magnetic field fulfilling the resonance condition in the latter case. The main discharge and H^- production volumes are decoupled from each other by an electrostatic [30] or magnetic [31] filter (the latter being a typical solution), which reduces the average energy of the electrons diffusing from the driver region to the H^- production region, thus favoring DEA over other molecular processes, e.g. electronic excitation, and decreasing the probability of H^- stripping by hot electrons.

The operation of the electrostatic filter is based on a negatively biased mesh immersed into the plasma. The obvious benefit of electrostatic filtering is that the fraction of the electron population passing through the filter can be actively tuned by adjusting its potential. Furthermore, the conducting grid prevents unwanted leakage of

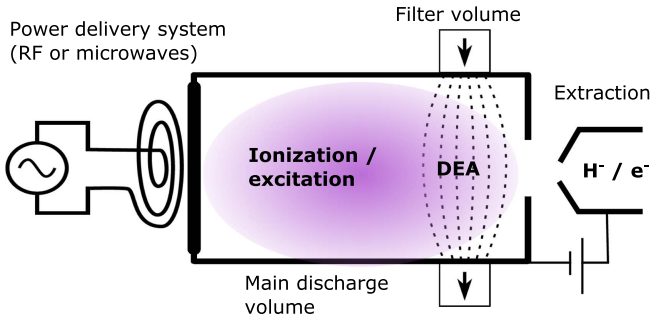

Figure 2. Schematic illustration of the mechanical design of typical RF (or ECR) volume production H^- ion source.

the electromagnetic radiation from the driver region into the H^- production region [32]. However, the drawback of the electrostatic filter is that only the high-energy tail of the initial EED in the driver-region is utilized for the DEA as the majority of the electrons are repelled by the negative potential of the grid. In addition, it is questionable whether such perforated plate can work effectively at high plasma densities i.e. when the plasma sheath thickness becomes significantly smaller in comparison to the dimensions of the apertures [33]. The operation of the magnetic filter is based on diffusion of electrons in transverse magnetic field, discussed thoroughly e.g. in [34], and the resulting decrease of the average electron energy in the H^- production volume (see e.g. [35] for experimental verification). The filter field is typically realized by using permanent magnets in dipole configuration. The optimum strength of the filter field depends on the EED as well as the mechanical design of the ion source. The optimization of the filter field is more complex in the case of ECR-driven ion sources (in comparison to RF-driven sources) because the plasma heating mechanism sets requirements to the magnetic field strength and topology i.e. coupling the driver region to magnetic filter and H^- production region could be challenging. This is especially true for ion sources utilizing solenoid field in the driver region. In such configuration the use of electrostatic filter has been favored in some cases [30]. It is also possible to utilize the topology of the magnetic field for filtering hot electrons as described e.g. in [36].

In order to extract negative ions, the ion source is biased to a negative potential with respect to the subsequent beamline. Co-extracted electrons are an inherent feature of all plasma discharge H^- ion sources. Therefore, special attention must be paid on the measurement of the H^- current to assure that the detected beam current is not plagued by electrons. It has been observed that in RF and ECR sources operating in volume production mode the e/H^--ratio of the extracted negative beam (10–100) is typically higher than in arc discharge sources (<10) [20, 37–40]. Thus, controlled dumping of the parasitic electron current to the extraction electrodes is more challenging in these cases. Moreover, the high co-extracted electron current can affect the transport of the extracted beam due to space charge effects. Estimating the co-extracted electron current can be difficult especially if the electrons are magnetically deflected from the extracted beam at low energy. It has been shown that in such cases they can drift in the extraction region and impinge back on the plasma electrode [41], which could result to underestimating the e/H^--ratio.

5. RF H^- ion sources

Inductively coupled RF ion sources relying to the volume production of H^- ions can be operated either in pulsed or continuous (cw) mode depending on the application and desired beam current. Pulsed operation is realized by chopping the RF power, which means that pulsed and cw sources typically operate under somewhat different neutral gas pressures as reliable plasma breakdown requires higher neutral gas density. High-performance RF volume production sources typically reach power efficiencies up to 1 mA kW^{-1}. In cw operation thermal effects often limit the maximum tolerable RF power coupled into the plasma through the transparent window to $\leqslant 5$ kW whereas pulsed sources can be operated with several tens of kW of RF power at $\leqslant 10\%$ duty factor. Altogether, the optimization procedure of pulsed and cw sources is different; cw operation allows the operator more flexibility to adjust the neutral gas pressure while pulsed sources are typically optimized by the brute force approach, namely by increasing the RF power.

5.1. Pulsed RF H^- volume production ion sources

RF ion sources relying on volume production of H^- are typically operated in continuous mode. Pulsed operation allows replenishing the cesium coverage between the discharge pulses which effectively inundates the

benefits of the volume production. Thus, pulsed high-current RF H^- sources are rarely found. There are however, two well-documented exceptions to this trend. The HERA RF volume source developed at DESY [22, 42–44], has routinely delivered an H^- current of 40mA at 8 Hz with short pulses using an RF power of 20 kW at 2 MHz. The highest reported H^- current extracted from the HERA source is 60 mA in $\leqslant$200 μs pulses [42]. In long pulse operation, i.e. 3 ms pulses, the source has delivered 30–40 mA of H^-, with approximately 30% current droop over the pulse [43]. The design of the source features an external antenna wound around a ceramic (Al_2O_3) plasma chamber and a collar structure extruding inwards from the plasma electrode [44].

The HERA ion source design was later adopted to CERN as a prototype of the Linac4 H^- ion source. The source did not, however, meet the performance goals of the Linac4 project as the electrons, co-extracted with the H^- and dumped onto the extraction electrode at 45 kV, caused severe structural damage. Later an improved design of the ion source demonstrated H^- beam current of 20 mA with an e/H^--ratio of 50–60 in volume production mode with 30 kW of RF power [39]. Further developments at CERN have lead into a redesign of the HERA ion source concept and resulting to 30mA of H^- current (e/H^--ratio of 20) at 45 keV produced with 30 kW of RF power in 500 μs pulses [39]. However, the performance goal of the Linac4 project is 80 mA of H^- and it is considered unlikely to achieve this level with a volume source. Therefore, the recent research activities at CERN have been focused on cesiated operation of the RF ion source [45] causing the volume source development at CERN to become stagnant.

5.2. CW RF H^- volume production ion sources

In continuous operation mode maintaining an optimum cesium coverage is at least challenging if not impossible and the volume production becomes the preferred choice. Thus, several cw RF ion sources relying on volume production of H^- have been developed and reported e.g. in [23, 46–48].

To our knowledge the first truly successful effort has taken place at Seoul National University (SNU) where the 13.56 MHz RF-driven source has produced 1.2 mA of H^- in cw mode with a power efficiency of approximately 1 mA kW^{-1} [23, 49]. The SNU RF ion source was used for an interesting experiment in which the plasma electrode was covered with different materials, namely tantalum, molybdenum and stainless steel [49]. The H^- currents obtained with tantalum were significantly higher in comparison to other materials, which underlines the contribution of surface processes to the volume production of H^-.

Another example of an RF-driven H^- ion source exceeding 1 mA of H^- current is the RADIS (RADiofrequency Ion Source) developed at the University of Jyväskylä (JYFL). The RADIS source and the JYFL test stand for negative ion source development are shown in figure 3. The RF system of the RADIS ion source consists of a 5 kW 13.56 MHz amplifier connected to a flat spiral antenna via a capacitive matching circuit with two adjustable vacuum capacitors. The power is coupled into the ion source through a ceramic (AlN) 6 mm thick window. The plasma chamber is surrounded by permanent magnet rows forming a 16-pole multicusp field for plasma confinement. The magnetic filter field is generated either by a set of two electromagnet coils or permanent magnet bars depending on the desired configuration. The H^- beam and parasitic electrons are extracted through $\phi = 7$ mm opening in the biased plasma electrode and accelerated by the potential difference between the plasma electrode and the puller electrode. The beam is then decelerated and the electrons are dumped into a water-cooled (copper) dump housing a set of permanent 'electron-dump magnets'. Finally, the ~20 keV beam is focused by a symmetric accelerating einzel lens. The beam current is first measured from a Faraday cup (FC1) approximately 300 mm downstream from the extraction. In order to assure that the measured beam current is not affected by co-extracted electrons or secondary electrons emitted from the extraction electrodes, the beam passing the first diagnostics chamber is deflected by a transverse magnetic field and finally measured at the end of the test stand from another Faraday cup (FC2) approximately 500 mm downstream from the first cup. Typically the readings of the two Faraday cups differ by approximately 10%–20% which is believed to be due to secondary electrons measured by FC1 and/or stripping of H^- by collisions with the neutral gas within the drift space between FC1 and FC2.

Originally the RADIS ion source was equipped with an electromagnet producing an adjustable filter field. The optimum field strength was found to be approximately 25 mT resulting to 1 mA of H^- with 3 kW of rf power and e/H^--ratio of 15–25 [40]. It was, however, observed that the mechanical structure housing the magnet coils and the resulting magnetic field topology were restricting the plasma density near the extraction aperture. Consequently the electromagnet filter was replaced with permanent magnets. The strength of the filter field was then optimized experimentally [48] resulting to an improvement of the power efficiency i.e. 1mA beam current with 1.75 kW of RF power. It is worth noting that the original (electromagnet) configuration provided better control over the e/H^--ratio. The highest obtained H^- beam current of 1.3 mA (with 2.5 kW) exceeds the 1 mA design specification of the RADIS ion source intended to replace a filament-driven ion source serving as an injector of the MCC30-cyclotron at JYFL. Additional (ongoing) improvements are, however, required as the long-term reliability of the ion source is compromized by overheating and limited voltage holding of the

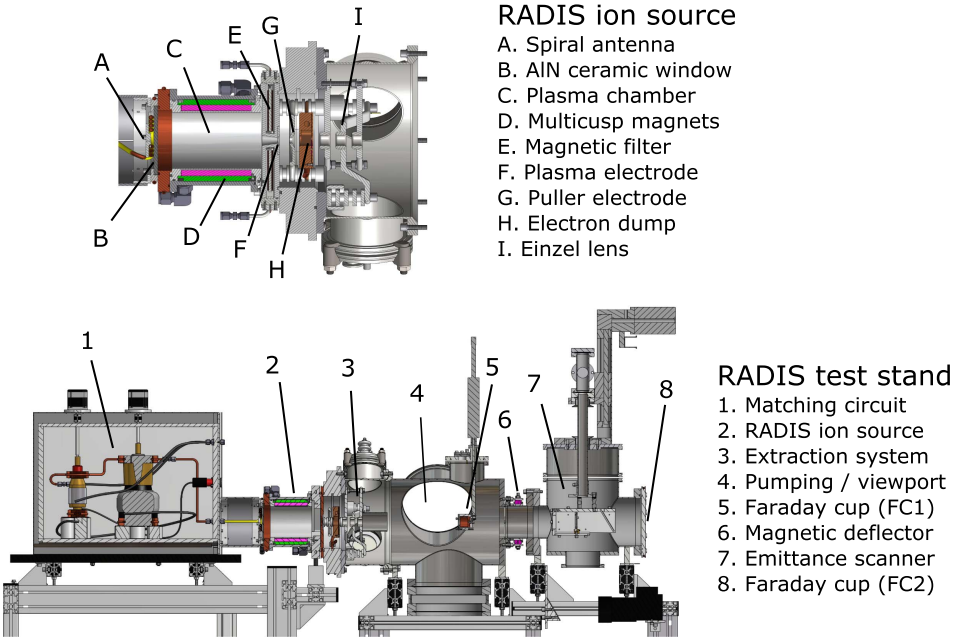

Figure 3. The RADIS ion source and the negative RF ion source test stand at JYFL.

extraction electrodes, especially the accelerating einzel lens. Further planned developments include introducing tantalum into the surfaces of the RADIS plasma chamber and injection of small quantities of xenon gas into the discharge, which has been demonstrated to improve the H^- volume production [46].

Recently the RF system developed for the RADIS ion source was coupled with the plasma chamber, magnetic filter and extraction system of the TRIUMF-type (filament) ion source [50] at the ion source test facility (ISTF) operated by D-Pace Inc. [51]. The results of the first experimental campaign are reported in [52] and summarized hereafter. The highest H^- beam current was 6.1mA at 30 keV with 2.7 kW of RF power. The beam was extracted through $\phi = 14$ mm aperture resulting to 4-rms emittance of 0.41 mm mrad (containing 85% of the beam) and estimated e/H^--ratio of approximately 7. The obtained H^- beam current density of approximately 1.5 mA cm^{-2} per kW of RF power is comparable to the corresponding figure of approximately 1.4 mA cm^{-2} per kW of RF power, obtained with the RADIS source at JYFL. The experiments at the ISTF allow comparing the power efficiencies of the arc discharge and the RF discharge. The TRIUMF ion source has been reported to reach 6 mA of H^- with 1 kW of RF power [35], which implies that the arc discharge is approximately 2.5 times more power efficient in terms of H^- production. Furthermore, it was observed that in the RF-mode of operation the optimum plasma electrode potential was between 20 and 25 V, which is considerably higher than what is usually applied to the electrode when the filament-powered version of the source is used (3–4 V) [52]. The value of approximately 20 V is consistent with the experience obtained with the RADIS source at JYFL.

6. 2.45 GHz ECR H^- ion sources

Microwave-driven plasma generators, which may be classified as 2.45 GHz ECR ion sources, have demonstrated their efficiency, reliability and reproducibility for the production of positive light ion beams, e.g. H^+ and D^+, both in cw and pulsed operation. The maintenance effort required to operate such ion sources is minimal due to the lack of consumable parts. Several attempts to design and construct H^- ion sources based on ECR discharge have been reported world-wide. The pioneering experiments with a 2.45 GHz microwave-driven H^- ion source producing mere 1 μA ion beam are reported in [53]. Since then several variants of microwave-driven H^- ion sources including, for example, so-called HYBRIS ion source (utilizing the 2.45GHz hydrogen discharge as a plasma cathode) [54], coaxial-antenna ion source developed at CERN [55] and dipolar plasma generators [36], have been reported. Nevertheless, attempts to develop microwave-driven H^- ion sources have typically become stuck at beam currents below 1mA level. Ion source teams working at Argonne National Laboratory and CEA/Saclay reporting beam currents of 5 mA [56, 57] and 3.8 mA [30], respectively, have been the first ones to overcome the mA-milestone. However, until 2013 there are no publications reporting more than a few mA of H^- beam produced with a microwave-driven source [58]. The situation has changed drastically with the development of the microwave H^- ion source at Peking University (PKU) discussed hereafter.

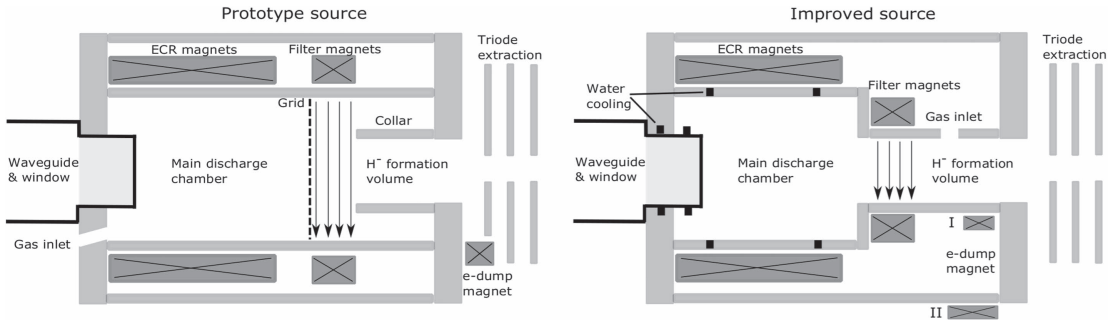

Figure 4. A schematic presentation of the PKU prototype and improved sources.

6.1. The PKU prototype H^- ion source

For more than three decades, the PKU ion source group has undertaken a research and development program on high current single charge ion beams, including H^+ and D^+ [59] as well as molecular ion beams including H_2^+ and H_3^+ [60], with compact permanent magnet 2.45 GHz electron cyclotron resonance (PMECR) plasma generators. In 2012, the PKU group designed the first permanent magnet (uncesiated) volume production H^- ion source [61] based on the 2.45 GHz PMECR microwave discharge, which already had demonstrated a proton beam current of 100 mA at 50 keV. The main modifications were made on the structure of the plasma chamber and the configuration of magnetic field at different regions of the discharge volume. The scheme of electron dumping was also developed at this stage. The PKU prototype H^- ion source is shown schematically in figure 4.

The source body is physically separated into three sections. The first section adjacent to the microwave coupling system is the primary ionization chamber where high temperature electrons heated by the microwave electric field interact with hydrogen molecules ionizing, dissociating and vibrationally exciting them. The magnetic field fulfilling the resonance condition, i.e. $B = 87.5$ mT, is generated by a set of permanent magnet rings magnetized in axial direction. The microwave coupling between the rectangular waveguide (WR340) and the cylindrical plasma chamber is realized through a ceramic microwave window, which serves also as a vacuum break, as described in [62]. The second part is the magnetic filter zone realized by generating a transverse 10 mT dipole magnetic field with permanent magnets placed outside the vacuum chamber. A tungsten grid (~1 mm wire diameter, 5 mm wire spacing) is installed into the filter region to block microwaves and thereby limiting electron heating in the H^- production volume. The grid is mounted with a cylindrical liner and its position can be changed for optimizing the H^- production. The optimum location has been found to be 25 mm measured from the plasma electrode. The third section is the H^- formation region where the vibrationally excited H_2 molecules that drift from the main discharge interact with cold electrons, which diffuse through the magnetic filter, generate H^- ions by DEA. In order to improve the H^- production efficiency, a stainless steel cylinder is used as a collar in the H^- formation part. A permanent magnet block, magnetized parallel to the filter field direction, is positioned outside beam formation volume which makes it possible to dump the electrons before the H^- beam is formed. An uncooled stainless steel triode system developed for 50 kV positive ion beam extraction system was used for H^- extraction through a 6 mm aperture and subsequent beam formation. The voltage of the intermediate electrode was set to +2 kV throughout the experiments summarized here.

The extraction system is followed by a large vacuum chamber housing a Faraday cup (FC1) and a multi-slit single-wire emittance scanner at a distance of approximately 300 mm from the extraction aperture. At the location of the wire scanner the beam spot size is typically 50–60 mm (FWHM). The extracted beam is analyzed with a 90 degree bending magnet ($r = 270$ mm) located 600 mm downstream from FC1. The beam exiting the magnet drifts another 400 mm before it is detected by another Faraday cup (FC2). Both Faraday cups are equipped with secondary electron suppression. Because the FC1 current signal consists of both, H^- and electrons, the H^- beam current and e/H^--ratio can not be measured directly. On the other hand, all extracted H^- ions are not transported through the drift sections and the bending magnet. Therefore, all the currents reported originally in [61, 63–65] and summarized hereafter are measured as follows: (1) the total negative beam current I_{beam} is measured from FC1, (2) H^- and electron signals (U_{H^-} and U_e) are recorded from FC2 and (3) the H^- current and e/H^--ratio are calculated using their relative fractions at FC2 multiplied by the total current measured at FC1, i.e. $I_{H^-} = \frac{U_{H^-}}{U_{H^-} + U_e} I_{beam}$ and $e/H^- = \frac{U_e}{U_{H^-}}$.

A pulsed (100 Hz / 1 ms) H^- beam of 15 mA at 40 keV was obtained just two weeks since the beginning of the experiments with 1.8 kW of pulsed microwave power. The operation of the prototype source was impeded by breakdowns between the extraction electrodes as they were damaged by the deflected electron beam. The prototype source was not operated in cw mode before the damage occurred.

6.2. Improved versions of the PKU H^- ion source

In order to overcome the problems related to the extraction system of the prototype, a new version of the PKU H^- ion source [63–65] was designed in 2013. Improvements were focused on the location of the gas injection, microwave blocking method, electron dumping, and the structure of the extraction system. The improved design is shown schematically in figure 4. Based on a previous study [64] the location of the gas injection was moved from the main discharge volume near the microwave window to the H^- formation volume. In order to improve the structural properties of the microwave blocking grid, the plasma chamber size around the magnetic filter was shrank to match the size of the collar so that the resulting sharp boundary between the main discharge and the filter volume stops the microwave radiation and makes the tungsten grid redundant. This edge also affects the neutral gas distribution in the discharge volume. Furthermore, tantalum sheets were inserted into the plasma chamber of the modified ion source. To lower the load of the extraction high voltage power supply and to better protect the electrodes, the electron dumping scheme was changed so that the electron trajectories are deflected within the collar, which reduces their contribution to the extracted beam. This was realized with a permanent magnet block embedded outside the second chamber, either at location I or II in figure 4. A new water-cooled molybdenum triode extraction system was designed for the H^- beam formation. The dimensions of the source body are about ϕ 116 mm $\times$ 124 mm. The whole ion source, including the source body, 50 kV extraction system and microwave coupling section, is confined within a volume of ϕ 310 mm $\times$ 180 mm.

Four sources, referred later as source numbers 1–4, with different water cooling arrangements were fabricated based on the new design. All sources can be operated in pulsed and cw mode with a (microwave) duty factor varying in the range of 1%–100%. Sources (number 3 and 4) which have better cooling properties perform better in comparison to those with limited cooling capacity (number 1 and 2) [65]. The best result obtained with source number 3 is 35 mA of H^- with a duty factor of 10% (100 Hz/1ms) and 25 mA of H^- in cw mode at 35 keV. The rms emittance of the 35 mA/35 keV H^- beam at 10% duty factor has been measured to be 0.195 π mm mrad. The power efficiency changes from 7 mA/kW to 20 mA/kW when the duty factor changes from 1% to 100%. With source number 4, the best result obtained so far is 25 mA/35 keV at 1000 W microwave power in cw mode. The corresponding power efficiency is about 25 mA kW^{-1}, which is much higher than that of source number 3. In pulsed mode the H^- current increases from 29 to 35 mA and the power efficiency from 16.1 to 19.4 mA kW^{-1} with the duty factor increasing from 1% to 20%. The difference between sources 3 and 4 may be caused by the slight difference of magnetic field around the source body [65]. Just recently several improvements such as added water-cooling around the source body, optimized electron dumping magnet configuration and implementation of optimum operating parameters, were carried out on source number 4. These modifications resulted to H^- current of 45 mA at 35 keV in pulsed mode with 10% duty factor (100 Hz/1 ms) and 2.1 kW microwave power as well as 29 mA H^- current in cw mode with 1 kW power [66]. The corresponding e/H^--ratios measured as described above are 0.29 (pulsed) and 0.21 (cw), respectively. These exceptionally low e/H^--ratios of the transported beam could be explained by electrons being deflected already in the H^- formation volume and, thereby, not transported efficiently to the current measurement (similar to [41]). This explanation is supported by the fact that the modification of the electron dumping scheme resulted to lower e/H^--ratio in comparison to the prototype source.

The source number 2 producing 20 mA with 100 Hz/10% duty factor will be used to deliver pulsed H^- beam for Space Radio-Environment Simulate Assembly project (SPRESA) and source number 3 will generate cw H^- beam for a cyclotron used for PET isotope production.

7. Discussion

The performance levels of various RF/ECR H^- volume production ion sources reported in the literature are summarized in table 1. Only those ion sources producing beam currents $\geqslant$ 1 mA have been included.

The benefits of volume production sources are highlighted in cw operation in which the use of cesium for surface enhanced H^- production is complicated if not impossible. The values summarized in table 1 indicate that ion sources based on ECR-driven plasmas outperform those based on inductive RF-disharges. Somewhat surprisingly the reported performance of the 2.45 GHz H^- ion source developed at PKU exceeds the performances of other ECR-based H^- ion sources by almost an order of magnitude. The results, i.e. the extracted beam currents, e/H^--ratios and especially the remarkably good power efficiencies that cannot be explained solely by volumetric plasma processes, imply that the surface processes contributing to the H^- volume production are not fully understood nor optimized. The situation calls for employing plasma diagnostics techniques, e.g. VUV-spectroscopy probing the volumetric excitation rate to $B^1\Sigma_u^+$ and $C^1\Pi_u$ singlet states [29] and laser photodetachment probing the H^- density [67], to study the PKU ion sources. It must be emphasized that the reported H^- currents (or e/H^--ratios) of the ANL and PKU sources are not measured directly and, therefore, further experiments validating the results are necessary. The reported H^- beam currents of the ECR-

Table 1. Performances of RF/ECR H^- volume production ion sources as reported in the literature. Some data, e.g. e/H^--ratios or pulse lengths/repetition rates that are not reported unequivocally have been omitted from the table.

Ion source	RF/ECR	I_{H^-} (mA)	e/H^-	Mode	References
HERA (DESY)	RF	40	26	20 kW, 8 Hz / 0.12%	[43]
		60	—	$\leqslant$200 μs pulses	[43]
		30–40	—	3ms pulses	[43]
DESY at CERN	RF	20	57	30 kW, 500 μs pulses	[39]
CERN IS01	RF	20	60	45 kW, 500 μs pulses	[39]
CERN IS02	RF	30	20	29 kW, 500 μs pulses	[39]
SNU	RF	1.2	—	1 kW, CW	[23]
RADIS (JYFL)	RF	1.3	20–30	2.5 kW, CW	[48]
RADIS/TRIUMF	RF	6.1	7	2.7 kW, CW	[52]
ANL	ECR	4-5	—	700 W, CW	[57]
ECRIN (CEA)	ECR	3.8	—	1.2 kW, 10 Hz/10 ms	[30]
PKU prototype	ECR	15	—	1.8 kW, 100 Hz/1 ms	[61]
PKU source #4	ECR	45	0.29	2.1 kW, 100 Hz/1 ms	[66]
		29	0.21	1 kW, CW	[66]

driven sources are comparable to state-of-the-art filament-driven arc discharge sources producing up to 15 mA of H^- in cw mode [50]. The cw performance of RF ion sources has not yet reached this level the main challenge being lower power efficiency and higher e/H^--ratio in comparison to arc discharge ion sources.

Acknowledgments

This work has been supported by the EU 7th framework programme 'Integrating Activities—Transnational Access', project number: 262010 (ENSAR), the Academy of Finland under the Finnish Centre of Excellence Programme 2012–2017 (Nuclear and Accelerator Based Physics Research at JYFL), the State Key Laboratory of Nuclear Physics and Technology (Peking University) and National Science Foundation of China (Grant numbers 11305004 and 11575013). O T acknowledges the contributions of J Lettry, R Welton, T Kalvas and M Napari for their help in collecting the data and producing the figures. S X Peng acknowledges fruitful discussions with X L Guan, M Stockli and R Gobin.

References

[1] Moehs D, Peters J and Sherman J 2005 *IEEE Trans. Plasma Sci.* **33** 1786
[2] Fantz U *et al* 2008 *Rev. Sci. Instrum.* **79** 02A511
[3] Dimov G I 1996 *Rev. Sci. Instrum.* **67** 3393
[4] Belchenko Y I, Dimov G I and Dudnikov V G 1974 *Nucl. Fusion* **14** 113
[5] Bacal M and Hamilton G W 1979 *Phys. Rev. Lett.* **42** 1538
[6] Bacal M and Wada M 2015 *Appl. Phys. Rev.* **2** 021305
[7] Janev R K, Reiter D and Samm U 2003 *Collision Processes in Low-Temperature Hydrogen Plasmas* (*Berichte des Forschungszentrums Jülich* vol JUEL-4105) (Jülich: Forschungszentrum, Zentralbibliothek) (http://www.eirene.de/report_4105.pdf)
[8] Wadehra J M 1984 *Phys. Rev.* A **29** 106
[9] Wadehra J M 1979 *Appl. Phys. Lett.* **35** 917
[10] Capitelli M *et al* 2006 *Nucl. Fusion* **46** S260–74
[11] Mosbach T 2005 *Plasma Sources Sci. Technol.* **14** 610
[12] Hiskes J R 1980 *J. Appl. Phys.* **51** 4592
[13] Fantz U and Wünderlich D 2006 *At. Data Nucl. Data* **92** 853
[14] Hiskes J R and Karo A M 1990 *J. Appl. Phys.* **67** 6621
[15] Hall R I, Cadez I, Landau M, Pichou F and Schermann C 1988 *Phys. Rev. Lett.* **60** 337
[16] Capitelli M, Colonna G and D'Angola A 2016 *Fundamental Aspects of Plasma Chemical Physics—Kinetics* (New York: Springer)
[17] Bacal M, Hatayama A and Peters J 2005 *IEEE Trans. Plasma Sci.* **33** 1845
[18] Bretagne J, Delouya G, Gorse C, Capitelli M and Bacal M 1985 *J. Phys. D: Appl. Phys.* **18** 811
[19] Lieberman M A and Lichtenberg A J 2005 *Principles of Plasma Discharges and Materials Processing* 2nd edn (New York: Wiley)
[20] Leung K N, DeVries G J, DiVergilio W F, Hamm R W, Hauck C A, Kunkel W B, McDonald D S and Williams M D 1991 *Rev. Sci. Instrum.* **62** 100
[21] Keller R, Thomae R, Stockli M and Welton R 2002 *AIP Conf. Proc.* **639** 47
[22] Peters J 2002 *Proc. 21st Linear Accelerator Conference (LINAC) (Gyeongju, Korea)* p 42 (www.jacow.org)
[23] An Y, Jung B and Hwang Y S 2010 *Rev. Sci. Instrum.* **81** 02A702
[24] Gammino S, Celona L, Ciavola G, Maimone F and Mascali D 2010 *Rev. Sci. Instrum.* **81** 02B313
[25] Williamson M C, Lichtenberg A J and Lieberman M A 1992 *J. Appl. Phys.* **72** 3924
[26] Sakudo N 2000 *Rev. Sci. Instrum.* **71** 1016
[27] Aleiferis S and Svarnas P 2014 *Rev. Sci. Instrum.* **85** 123504

[28] Komppula J, Tarvainen O, Kalvas T, Koivisto H, Kronholm R, Laulainen J and Myllyperkiö P 2015 *J. Phys. D Appl. Phys.* **48** 365201
[29] Komppula J and Tarvainen O 2015 *Plasma Sources Sci. Technol.* **24** 045008
[30] Gobin R, Auvray P, Bacal M, Breton J, Delferriere O, Harrault F, Ivanov A A Jr, Svarnas P and Tuske O 2006 *Nucl. Fusion* **46** S281–6
[31] Leung K N and Bacal M 1984 *Rev. Sci. Instrum.* **55** 338
[32] Tuske O, Charruau G, Delferriere O, De Menezes D, Gobin R, Gauthier Y, Harrault F and Madur A 2007 *AIP Conf. Proc.* **925** 114
[33] Hong J I, Seo S H, Kim S S, Yoon N S, Chang C S and Chang H Y 1999 *Phys. Plasmas* **6** 1017
[34] Boeuf J P, Chaudhury B and Garrigues L 2012 *Phys. Plasmas* **19** 113509
[35] Hwang Y S, Cojocaru G, Yuan D, McDonald M, Jayamanna K, Kim G H and Dutto G 2006 *Rev. Sci. Instrum.* **77** 03A509
[36] Aleiferis S, Svarnas P, Tsiroudis I, Bechu S, Bacal M and Lacoste A 2014 *IEEE Trans. Plasma Sci.* **42** 2828
[37] El Balghiti-Sube F, Baksht F G and Bacal M 1996 *Rev. Sci. Instrum.* **67** 2221
[38] McAdams R, King R F and Newman A F 1990 *Rev. Sci. Instrum.* **61** 2176
[39] Lettry J *et al* 2015 *AIP Conf. Proc.* **1655** 030005
[40] Kalvas T, Tarvainen O, Komppula J, Koivisto H, Tuunanen J, Potkins D, Stewart T and Dehnel M P 2015 *AIP Conf. Proc.* **1655** 030015
[41] Kalvas T 2013 Development and use of computational tools for modelling negative hydrogen ion source extraction systems *PhD Thesis* University of Jyväskylä (http://urn.fi/URN:ISBN:978-951-39-5421-5)
[42] Peters J 2005 *Proc. Particle Accelerator Conference (PAC) (Knoxville, TN, USA)* p 788 (www.jacow.org)
[43] Peters J 2007 *AIP Conf. Proc.* **925** 79
[44] Peters J 2008 *Rev. Sci. Instrum.* **79** 02A515
[45] Lettry J *et al* 2016 *Rev. Sci. Instrum.* **87** 02B139
[46] Kalvas T, Hahto S K, Vainionpää J H, Leung K N, Wilde S B and Mandrillon P 2007 *AIP Conf. Proc.* **925** 136
[47] Zakcs J, Turner I, Day I, Flinders K, Crowley B and McAdams R 2015 *AIP Conf. Proc.* **1655** 030012
[48] Kalvas T, Tarvainen O, Komppula J, Koivisto H, Tuunanen J, Potkins D, Stewart T and Dehnel M 2016 *Rev. Sci. Instrum.* **87** 02B102
[49] An Y, Cho W, Chung K-J, Lee K, Jang S, Lee S-G and Hwang Y S 2012 *Rev. Sci. Instrum.* **83** 02A727
[50] Kuo T, Yuan D, Jayamanna K, McDonald M, Baartman R, Schmor P and Dutto G 1996 *Rev. Sci. Instrum.* **67** 1314
[51] Melanson S *et al* 2016 *Rev. Sci. Instrum* **87** 02B109
[52] Melanson S *et al Proc. 5th Int. Symp. on Negative Ions, Beams and Sources (Oxford, UK, September 2016)* (to be published)
[53] Marinak M M and Morse E C 1990 *Rev. Sci. Instrum.* **61** 508
[54] Keller R, Kwan J, Hahto S, Regis M and Wallig J 2007 *AIP Conf. Proc.* **925** 164
[55] Küchler D, Meinschad Th, Peters J and Scrivens R 2007 *AIP Conf. Proc.* **925** 121
[56] Spence D, Lykke K R and McMichael G E 1996 *Proc. 18th Linear Accelerator Conference (LINAC) (Geneva, Switzerland)* p 71 (www.jacow.org)
[57] Spence D and Lykke K R 1998 *Proc. 19th Linear Accelerator Conference (LINAC) (Chicago, IL, USA)* TU4048 (www.jacow.org)
[58] Stockli M P and Nakagawa T 2013 *Rev. Accel. Sci. Technol.* **6** 197
[59] Ren H T, Peng S X, Lu P N, Yan S, Zhou Q F, Zhao J, Yuan Z X, Guo Z Y and Chen J E 2012 *Rev. Sci. Instrum.* **83** 02B905
[60] Xu Y, Peng S X, Ren H T, Zhao J, Chen J, Zhang A L, Zhang T, Guo Z Y and Chen J E 2014 *Rev. Sci. Instrum.* **85** 02A943
[61] Ren H T *et al* 2013 *Proc. Int. Particle Accelerator Conference (IPAC'13) (Shanghai, China)* MOPFI034 (www.jacow.org)
[62] Song Z Z, Peng S X, Yu J X, Ming J C, Yuan Z X, Qian F and Guo Z Y 2006 *Rev. Sci. Instrum.* **77** 03A305
[63] Peng S X, Xu Y, Ren H T, Zhang T, Zhang A L, Zhang J F, Zhao J, Guo Z Y and Chen J E 2015 *Proc. Int. Particle Accelerator Conference (IPAC'15) (Richmond, VA, USA)* WEPWA027 (www.jacow.org)
[64] Peng S X, Zhang T, Ren H T, Zhang A L, Xu Y, Zhang J F, Guo Z Y and Chen J E 2016 *Rev. Sci. Instrum.* **87** 02B125
[65] Peng S X, Ren H T, Xu Y, Zhang T, Zhang A L, Zhang J F, Zhao J, Guo Z Y and Chen J E 2015 *AIP Conf. Proc.* **1655** 070005
[66] Zhang T, Peng S X, Ren H T, Zhang A L, Xu Y, Zhang J F, Wen J M, Guo Z Y and Chen J E *Proc. 5th Int. Symp. on Negative Ions, Beams and Sources (Oxford, UK, September 2016)* (to be published)
[67] Bacal M 2000 *Rev. Sci. Instrum.* **71** 3981